JCTC Journal of Chemical Theory and Computation

Article

pubs.acs.org/JCTC

# Benchmark Assessment of the Accuracy of Several van der Waals Density Functionals

Oleg A. Vydrov and Troy Van Voorhis*

Department of Chemistry, Massachusetts Institute of Technology, Cambridge, Massachusetts 02139, United States

**ABSTRACT:** The nonlocal correlation functional VV10, developed recently in our group, describes the whole range of dispersion interactions in a seamless and general fashion using only the electron density as input. The VV10 functional has a simple analytic form that can be adjusted for pairing with the exchange functional of choice. In this paper, we use several benchmark data sets of weakly interacting molecular complexes to test the accuracy of two VV10 variants, differing in their treatment of the exchange component. For the sake of comparison, several other density functionals suitable for noncovalent interactions were also tested against the same benchmarks. We find that the "default" version of VV10 with semilocal exchange gives very accurate geometries and binding energies for most van der Waals complexes but systematically overbinds hydrogen-bonded complexes. The alternative variant of VV10 with long-range corrected hybrid exchange performs exceptionally well for all types of weak bonding sampled in this study, including hydrogen bonds.

## 1. INTRODUCTION AND DESCRIPTION OF TESTED METHODS

In typical density functional theory (DFT) approximations, the correlation energy is expressed as a local or semilocal functional of the electron density. Such (semi)local approximations cannot describe long-range van der Waals (dispersion) interactions.[1] It has become common practice to augment DFT functionals with an empirical dispersion correction. A variety of such corrections have been developed, but most of them assume a pairwise atom−atom additive form.[1−4] To capture the proper physics of dispersion interactions within the formalism of Kohn−Sham DFT, the correlation energy must be expressed as a fully nonlocal functional of the density and/or orbitals.[5] Among the most computationally tractable and affordable nonlocal correlation models is the family of van der Waals density functionals (vdW-DF) introduced by Langreth and co-workers.[6−8] This family of functionals includes a few members developed in our group,[9−11] with the most recent addition, denoted as VV10, having a particularly simple construction.[10] VV10 is easy to implement, computationally efficient, and undemanding in terms of the basis set quality or the fineness of the numerical integration grid.[10] In this paper, we assess the performance of VV10 for weakly interacting molecular systems and compare its accuracy to several other promising DFT models.

We test three density functionals with nonlocal correlation components: vdW-DF2 of ref 8 and VV10 and LC-VV10 of ref 10. In all three of these methods, the exchange−correlation (xc) energy is represented as a sum of three parts:

$$E_{xc} = E_x + E_c^0 + E_c^{nl}$$

where the terms on the right-hand side are exchange, (semi)local correlation, and nonlocal correlation, respectively. In vdW-DF2, the refitted[12] version of Perdew−Wang-86 semilocal exchange[13] functional (denoted as rPW86) is used for $E_x$ and the local density approximation[14] correlation functional is used for $E_c^0$. In VV10 and LC-VV10, $E_c^0$ is described by the semilocal correlation functional of Perdew, Burke, and Ernzerhof (PBE).[15] VV10 uses the semilocal rPW86 exchange,[12] while in LC-VV10 the exchange component is described by a long-range corrected hybrid[16] LC-$\omega$PBE with the range-separation parameter $\omega = 0.45$ b$^{-1}$. The two versions of VV10 use slightly different parameters[10] in the nonlocal correlation component: the rPW86-based version of VV10 has $C = 0.0093$ and $b = 5.9$, whereas LC-VV10 has $C = 0.0089$ and $b = 6.3$. The parameter $C$ was fitted to give accurate asymptotic dispersion $C_6$ coefficients, while $b$ controls the short-range damping of nonlocal correlation.

All of the aforementioned nonlocal functionals have been implemented self-consistently[10,17] into the Q-CHEM software package.[18] Analytic energy gradients with respect to nuclear displacements are available,[10,17] thus enabling efficient geometry optimizations.

For the sake of comparison, we also included results obtained with two density functionals that contain no nonlocal correlation and therefore can be considered more "conventional": M06-2X of ref 19 and $\omega$B97X-D of ref 20. Both of these functionals contain a rather large number of empirical parameters that were fitted on training sets including weakly interacting systems. $\omega$B97X-D incorporates a force-field-like pairwise dispersion correction developed by Grimme.[2] M06-2X contains no long-range dispersion terms of any kind but was parametrized to mimic short- and intermediate-range dispersion effects.[19] The exchange component of $\omega$B97X-D has the form of a long-range corrected hybrid, while in M06-2X the Hartree−Fock exchange is admixed in a "global hybrid" fashion.

For our benchmark test sets, we use highly accurate reference data published or updated within the last year.[21−25] The errors reported in the tables are summarized with the help of mean signed errors (ME), mean absolute errors (MAE), mean signed percentage errors (MPE), and mean absolute percentage errors

**Received:** January 31, 2012
**Published:** April 13, 2012

(MAPE). We define binding energies as positive; therefore, a negative ME or MPE indicates an underbinding trend, while positive errors in interaction energies signify overbinding.

Practical usefulness of a computational method is determined as much by its accuracy as by its affordability in terms of computational expense. Nonlocal correlation components of vdW-DF2 and VV10 appreciably increase the cost of calculations but do not affect the overall computational scaling of a typical DFT implementation (see further discussion in ref 17). The actual cost of evaluating the nonlocal correlation terms depends very strongly on the choice of the numerical quadrature grid. With the computational details adopted in this study, the expense is quite moderate. In fact, the nonlocal correlation is not always the time-limiting step: when hybrid exchange is used, as in LC-VV10, the evaluation of the exact exchange component is typically the most time-consuming step.

## 2. TEST RESULTS

### 2.1. S66 Test Set of Equilibrium Interaction Energies.

Standard test sets of accurate benchmark data serve an important purpose for calibration and comparative assessment of newly developed computational methods. The recently published S66 test set[21,22] includes benchmark interaction energies for 66 weakly bound molecular complexes that represent typical intermolecular interaction motifs found in biomolecular structures. The S66 set is divided into three subsets: 23 hydrogen-bonded complexes, 23 dispersion-dominated complexes, and 20 others that exhibit some form of a mixed bonding character. The reference values of the binding energies were obtained at a high level of correlated wave function theory: the authors estimate[22] the residual uncertainty in the reference values to be under 1%.

We have calculated the binding energies for all systems in the S66 set using five density functional methods described in the introduction. The interaction energies are computed self-consistently with the aug-cc-pVTZ basis set and counterpoise corrected. The unpruned Euler−Maclaurin−Lebedev (75 302) quadrature grid was used to evaluate all local and semilocal contributions and the (50 194) grid was used for the nonlocal components. Table 1 summarizes deviations from the reference values[22] for binding energies computed at fixed equilibrium geometries from ref 21.

As can be seen by the sign of MPE in Table 1, vdW-DF2 tends to underbind on average. The underbinding tendency of vdW-DF2 is particularly pronounced for complexes where at least one of the monomers is aromatic. In terms of the average errors for the whole S66 set, vdW-DF2 is the worst performer among the five methods in Table 1.

VV10 consistently overbinds all hydrogen-bonded complexes in the S66 set. For the other two subsets of S66, VV10 also tends to overbind on average. Analysis of the errors for individual complexes reveals that the tendency of VV10 to overestimate equilibrium binding energies is more pronounced for systems of larger size. Among dispersion-dominated complexes, overbinding is quite strong for duplexes formed by two saturated hydrocarbons. The parameter $b$ in VV10 was fitted[10] to minimize the errors in equilibrium binding energies, but the training set was comprised of smaller (on average) systems than those in the S66 set. The main culprit of the uneven performance of VV10 for systems of different sizes is likely its semilocal rPW86 exchange component. The performance for S66 is substantially improved when a long-range corrected exchange functional is used: LC-VV10 yields the lowest total errors in Table 1 and exhibits a uniformly outstanding accuracy for all three subsets of S66.

**Table 1. Summary of Deviations from the Reference Values (Ref 22) of the Binding Energies for the S66 Test Set, Computed at Fixed Equilibrium Geometries from Ref 21[a]**

| | vdW-DF2 | VV10 | LC-VV10 | ωB97X-D | M06-2X |
|---|---|---|---|---|---|
| Hydrogen Bonds (23) | | | | | |
| MPE (%) | −5.6 | 6.4 | −0.4 | −0.4 | −3.3 |
| MAPE (%) | 5.8 | 6.4 | 2.3 | 2.2 | 3.9 |
| MAE | 0.62 | 0.53 | 0.20 | 0.16 | 0.32 |
| Dispersion (23) | | | | | |
| MPE (%) | −2.8 | 7.5 | −2.1 | 17.0 | −9.2 |
| MAPE (%) | 8.7 | 7.9 | 3.3 | 17.2 | 10.1 |
| MAE | 0.33 | 0.20 | 0.10 | 0.50 | 0.29 |
| Others (20) | | | | | |
| MPE (%) | −12.8 | 1.0 | 0.0 | 3.8 | −4.6 |
| MAPE (%) | 13.1 | 4.3 | 4.5 | 5.6 | 7.3 |
| MAE | 0.49 | 0.15 | 0.17 | 0.20 | 0.26 |
| Total (66) | | | | | |
| MPE (%) | −6.8 | 5.1 | −0.9 | 6.9 | −5.8 |
| MAPE (%) | 9.0 | 6.3 | 3.3 | 8.5 | 7.1 |
| MAE | 0.48 | 0.30 | 0.15 | 0.29 | 0.29 |

[a]All calculations were performed self-consistently with the aug-cc-pVTZ basis set and counterpoise corrected. MPE and MAPE are in percents, MAE is in kcal/mol.

Hujo and Grimme also recently applied VV10 to the S66 set.[26] For the standard version of VV10 (with rPW86 exchange and PBE correlation) they report a MAE of 0.45 kcal/mol, which is considerably larger than the MAE of 0.30 kcal/mol that we obtained for the same S66 test set. This discrepancy is caused in part by the difference in the adopted reference values: we used the numbers from ref 22, whereas Hujo and Grimme used the earlier values from ref 21. In addition, the implementation of Hujo and Grimme[26] lacks self-consistency, and computational details (such as the basis set and the numerical integration grid) are quite different from ours.

As Table 1 shows, ωB97X-D yields rather low errors for hydrogen bonds but performs poorly for the dispersion-dominated subset. ωB97X-D severely overbinds complexes of saturated hydrocarbons. For instance, the binding energy of cyclopentane−neopentane complex is overestimated by 40%. This overbinding tendency seems to stem from the dispersion correction included in ωB97X-D. The asymptotic $C_6$ coefficients used in ωB97X-D were adopted from the "second-generation" empirical dispersion correction scheme by Grimme,[2] which assigns $C_6$ = 30.4 au (hartree·b$^6$) for all types of carbon−carbon interactions. For the less-polarizable saturated sp$^3$ carbon atoms, this $C_6$ value is clearly too large. In fact, the more recent "third-generation" dispersion correction (denoted DFT-D3) by Grimme and coworkers[3] uses a much smaller value of $C_6$ = 18.1 au for interactions between saturated (sp$^3$-hybrid) carbon atoms. It is not surprising that the more advanced DFT-D3 scheme performs rather well for the S66 test set.[27]

For hydrogen-bonded complexes, the functionals with long-range corrected hybrid exchange components (LC-VV10 and ωB97X-D) perform particularly well. Thus, proper treatment of exchange interactions appears to be especially important for the description of hydrogen bonds. We note that M06-2X was applied to the S66 set in ref 27 and the results agree reasonably well with ours. M06-2X gives a rather uniform MAE of about

0.3 kcal/mol for each of the three subsets, as well as for the whole S66 set.

**2.2. S66×1.25: Out-of-Equilibrium Interaction Energies.** For the complexes in the S66 test set, reference binding energies are available not only at the equilibrium geometries, but also for a number of configurations deformed out of equilibrium.[21,22] In this subsection we consider one such modified test set which we denote S66×1.25. The geometries of the systems in the S66×1.25 set are obtained from the equilibrium geometries by displacing the monomers away from each other, such that the minimum distance between them is 1.25 times the equilibrium value. The reference binding energies for the S66×1.25 complexes were calculated[21] at a somewhat lower level of theory, but the estimated uncertainty in the reference values is still under 3%. In Table 2 we summarize the errors obtained with five density functionals using the same computational details as in the previous subsection.

**Table 2. Summary of Deviations from the Reference Values of the Binding Energies for the S66×1.25 Test Set[a]**

| | vdW-DF2 | VV10 | LC-VV10 | ωB97X-D | M06-2X |
|---|---|---|---|---|---|
| Hydrogen Bonds (23) | | | | | |
| MPE | 3.6 | 4.6 | −0.3 | −0.9 | −4.8 |
| MAPE | 3.8 | 4.7 | 1.2 | 1.9 | 5.2 |
| Dispersion (23) | | | | | |
| MPE | 16.1 | 6.5 | −4.3 | 5.2 | −36.0 |
| MAPE | 16.1 | 6.5 | 4.5 | 5.2 | 36.0 |
| Others (20) | | | | | |
| MPE | 3.1 | −0.9 | −1.0 | 1.7 | −16.8 |
| MAPE | 7.0 | 2.9 | 2.9 | 2.9 | 16.8 |
| Total (66) | | | | | |
| MPE | 7.8 | 3.6 | −1.9 | 2.0 | −19.3 |
| MAPE | 9.1 | 4.8 | 2.9 | 3.4 | 19.4 |

[a]All calculations were performed self-consistently with the aug-cc-pVTZ basis set and counterpoise corrected. Geometries and reference binding energies are from ref 21. All numbers are in percent.

Comparing the MPEs in Table 1 to the MPEs in Table 2 for vdW-DF2, we observe a reversal of trends: from underbinding near equilibrium to overbinding at the S66×1.25 geometries. This result is not unexpected, since vdW-DF2 is known to give shifted binding energy curves with minima at somewhat too large intermonomer separations.[8,10]

Since the intermonomer distances in the S66×1.25 set are increased, the overlap between the electronic densities of the monomers is diminished. Hence the local and semilocal components of the exchange−correlation functionals are expected to have a smaller contribution to interaction energies, while contributions of long-range nonlocal interactions become relatively more significant. In this regard, it is worth noting that the percentage errors of VV10 decrease from S66 to S66×1.25. This may indicate that VV10 provides a satisfactory description of the long-range nonlocal correlations. A very different trend is exhibited by M06-2X: it performs reasonably well at equilibrium geometries (Table 1) but it strongly underbinds dispersion-dominated complexes in the S66×1.25 set (Table 2). Thus the lack of long-range dispersion terms in M06-2X becomes clearly detrimental when intermonomer distances are just 25% larger than equilibrium.

As Table 2 shows, both long-range corrected functionals, LC-VV10 and ωB97X-D, perform rather well for the S66×1.25 set. ωB97X-D yields significantly lower total percentage errors for the nonequilibrium S66×1.25 set (Table 2) as compared to the equilibrium geometries (Table 1).

**2.3. Binding Energy Curves for Benzene−$H_2S$ and Pyridine Dimer.** In ref 10 we computed interaction energy curves for several weakly bound complexes using VV10 and vdW-DF2. In this subsection we report the binding energy curves of two systems that were not included in our previous[10] study: the benzene−$H_2S$ complex of $C_{2v}$ symmetry and the pyridine dimer in the stacked sandwich-shaped configuration ($C_{2h}$ symmetry group). For both of these systems, very accurate reference data have been tabulated recently.[23] We used the same set of five functionals and the same computational details as for the S66 set above. We used the molecular geometries provided in ref 23. Counterpoise corrections were applied at all intermonomer distances. The results are presented in Figures 1 and 2. In both of these figures, the left panel displays the binding energy curves computed with VV10 and vdW-DF2—the two methods that incorporate the semilocal rPW86 exchange. The results shown in the right panel in Figures 1 and 2 correspond to the functionals with hybrid exchange components.

As Figure 1 shows, both VV10 and LC-VV10 yield very accurate interaction energies for benzene−$H_2S$ at all sampled

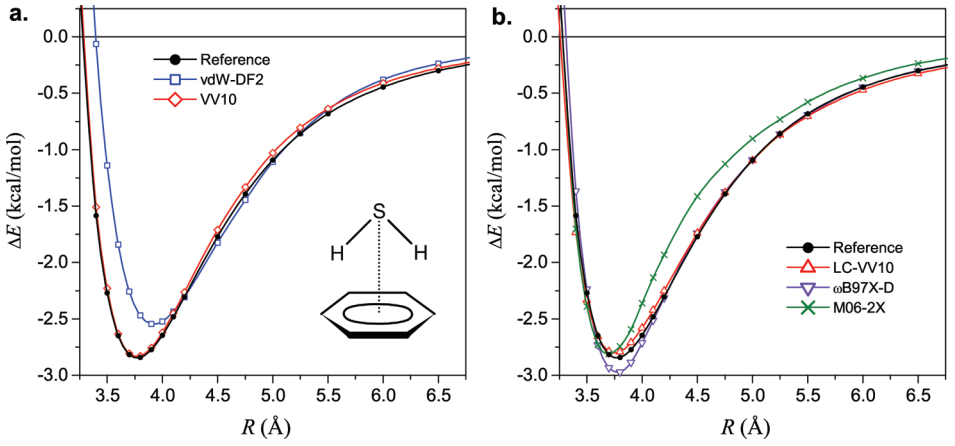


**Figure 1.** Interaction energy curves for the benzene−$H_2S$ complex, computed self-consistently with the aug-cc-pVTZ basis set. $R$ is the distance between the S atom and the benzene plane. Reference values are from ref 23.

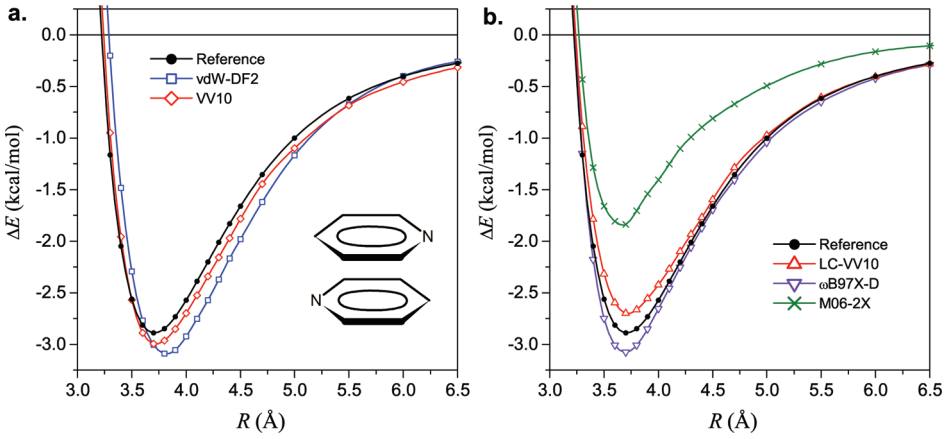


**Figure 2.** Interaction energy curves for the pyridine dimer in sandwich configuration, computed self-consistently with the aug-cc-pVTZ basis set. *R* is the separation between the monomer planes. Reference values are from ref 23.

**Table 3. Counterpoise-Corrected Dissociation Energies (in kcal/mol) for $CO_2$−X Complexes Computed with the aug-cc-pVQZ Basis Set[a]**

| complex | symm | ref | vdW-DF2 | VV10 | LC-VV10 | ωB97X-D | M06-2X |
|---|---|---|---|---|---|---|---|
| $CO_2$−Ar | $C_{2v}$ | 0.57 | 0.69 | 0.60 | 0.41 | 0.27 | 0.36 |
| $CO_2$−$N_2$ | $C_{2v}$ | 0.94 | 1.06 | 0.97 | 0.78 | 0.51 | 0.71 |
| $CO_2$−CO | $C_{2v}$ | 1.16 | 1.29 | 1.31 | 1.06 | 0.79 | 1.03 |
| $CO_2$−$H_2O$ | $C_{2v}$ | 2.92 | 2.83 | 2.84 | 2.81 | 2.17 | 3.13 |
| $CO_2$−$NH_3$ | $C_s$ | 3.04 | 3.06 | 3.33 | 3.02 | 2.71 | 3.32 |
| $(CO_2)_2$ T | $C_{2v}$ | 1.23 | 1.26 | 1.11 | 1.03 | 0.63 | 0.96 |
| $(CO_2)_2$ PD | $C_{2h}$ | 1.49 | 1.50 | 1.39 | 1.23 | 0.83 | 1.34 |
| | | MPE (%) | 6.6 | 1.7 | −13.0 | −37.0 | −12.6 |
| | | MAPE (%) | 7.4 | 7.2 | 13.0 | 37.0 | 17.3 |

[a]Molecular geometries are fully optimized in each method. Reference values are from refs 24 and 25.

**Table 4. Intermolecular Distances for $CO_2$−X Complexes[a]**

| complex | $R^b$ | ref | vdW-DF2 | VV10 | LC-VV10 | ωB97X-D | M06-2X |
|---|---|---|---|---|---|---|---|
| $CO_2$−Ar | C···Ar | 3.42 | 3.49 | 3.40 | 3.50 | 3.89 | 3.42 |
| $CO_2$−$N_2$ | C···N | 3.13 | 3.17 | 3.10 | 3.18 | 3.40 | 3.06 |
| $CO_2$−CO | C···C | 3.22 | 3.29 | 3.16 | 3.23 | 3.32 | 3.13 |
| $CO_2$−$H_2O$ | C···O | 2.76 | 2.84 | 2.76 | 2.77 | 2.83 | 2.68 |
| $CO_2$−$NH_3$ | C···N | 2.92 | 3.01 | 2.88 | 2.91 | 2.95 | 2.84 |
| $(CO_2)_2$T | C···O | 2.96 | 3.02 | 2.98 | 3.02 | 3.32 | 2.92 |
| $(CO_2)_2$PD | C···C | 3.51 | 3.65 | 3.54 | 3.58 | 3.79 | 3.37 |
| $(CO_2)_2$PD | ∠CCO | 58.9 | 57.6 | 58.8 | 58.4 | 57.8 | 59.3 |
| | | ME (Å)[c] | 0.08 | −0.01 | 0.04 | 0.23 | −0.07 |
| | | MAE (Å)[c] | 0.08 | 0.03 | 0.04 | 0.23 | 0.07 |

[a]Computational details are as in Table 3. [b]Interatomic distances (in Å) at equilibrium, plus the CCO angle (in deg) in the PD dimer. [c]Include only the distances and exclude the CCO angle in $(CO_2)_2$PD.

intermonomer distances. For the sandwich pyridine dimer (Figure 2), the equilibrium intermolecular separation is well-reproduced by both VV10 and LC-VV10, but the interaction energy near equilibrium is slightly overestimated by VV10 and somewhat underestimated by LC-VV10.

As has been observed previously,[8,10] vdW-DF2 yields binding energy curves that are much too repulsive at short-range and with energy minima shifted to larger distances as compared to the reference curves. These effects are clearly seen in Figures 1 and 2. The equilibrium binding energy given by vdW-DF2 is underestimated for benzene−$H_2S$ but overestimated for pyridine dimer.

For both systems shown in Figures 1 and 2, ωB97X-D reproduces the binding energy curves rather well at nearly all distances. For both complexes, the equilibrium intermonomer distance is predicted well by ωB97X-D, but there is a slight overbinding near equilibrium.

M06-2X gives reasonable equilibrium biding energy for benzene−$H_2S$, although the minimum is at a shorter distance as compared to the reference. As seen in Figure 1, M06-2X underestimates the interaction energies for $R > 3.7$ Å, but the underestimation is not very strong in this case, because the asymptotic interactions in benzene−$H_2S$ are dominated by electrostatic and induction contributions. Binding energy curves

for benzene−$H_2S$ obtained with M06-2X and a few other density functionals were previously reported in ref 28. M06-2X performs notably worse for the pyridine dimer: as Figure 2 shows, M06-2X strongly underbinds this sandwich-shaped complex at all intermonomer distances. This indicates that long-range dispersion interactions (missing in M06-2X) are crucial for the proper description of $\pi-\pi$ stacking in the pyridine dimer.

**2.4. Complexes of $CO_2$ with Small Molecules.** In this subsection, we consider a set of weakly bound complexes containing carbon dioxide. For all of these complexes, given in Table 3, very accurate equilibrium geometries and interaction energies are available, obtained at a high level of correlated wave function theory.[24,25] The test set in Table 3 includes two different configurations of the $CO_2$ dimer: T-shaped and parallel-displaced (PD). The set also includes five complexes of $CO_2$ with other molecules. All of these $CO_2$−X complexes have a T-shaped form with a nonhydrogen atom of the X molecule positioned on top of the carbon atom of $CO_2$. We have fully optimized the geometries of all the complexes and their constituent monomers using the aug-cc-pVQZ basis set. The (99 590) grid was used for semilocal xc components, while (75 302) was used for nonlocal correlation.

As Table 3 shows, the equilibrium binding energies of $CO_2$-containing duplexes are predicted quite accurately by vdW-DF2 and VV10 but systematically underestimated with LC-VV10 and $\omega$B97X-D. The underbinding in $\omega$B97X-D is not only systematic but also quite severe. M06-2X underestimates dissociation energies of most (but not all) complexes in Table 3.

Table 4 shows equilibrium intermonomer distances as predicted by each of the five tested functionals. It also includes the C−C−O angle in the parallel-displaced $CO_2$ dimer. VV10 yields very accurate geometries for all the complexes, and LC-VV10 performs almost equally well. Equilibrium intermolecular distances are systematically overestimated by both vdW-DF2 and $\omega$B97X-D, but the errors are much larger in $\omega$B97X-D. M06-2X yields intermonomer separations that are moderately but systematically underestimated.

The large systematic errors of $\omega$B97X-D for $CO_2$-containing complexes render it the worst performer among the methods included in Tables 3 and 4. The best performer for these systems is clearly VV10.

## 3. CONCLUSIONS

Among the five methods tested in this study, only M06-2X does not incorporate any long-range dispersion terms. However, M06-2X was fitted to mimic the effects of dispersion correlations at intermediate range, and in this respect it is among the best of its kind. Indeed, M06-2X often gives reasonably good interaction energies for van der Waals complexes near equilibrium geometries, where the monomer densities overlap substantially. At the same time, M06-2X gives large errors for complexes out of equilibrium, where the density overlap is diminished.

The inclusion of an explicit dispersion correction (as in $\omega$B97X-D) does not necessarily lead to improved performance for weakly bound complexes at equilibrium. In fact, in many of our tests we found $\omega$B97X-D to be inferior to M06-2X for near-equilibrium geometries. The parametrization of the empirical dispersion correction in $\omega$B97X-D may not be optimal and there is certainly room for improvement. Development of dispersion corrections is an active area of research and more flexible and elaborate models have already been proposed[3,4] and shown to perform rather well.[27]

The main focus of this paper was on the latest generation of seamless nonlocal correlation functionals. We have demonstrated that these van der Waals density functionals (vdW-DF2, VV10, and LC-VV10) provide a predictive power on par with the most accurate methods of comparable computational cost. In most of our benchmark assessments, VV10 and LC-VV10 emerged as best performers among the tested methods. The accuracy of VV10 for hydrogen bonds is not fully satisfactory, but the culprit appears to be the semilocal rPW86 exchange incorporated therein. The version with the long-range corrected hybrid exchange—LC-VV10—exhibits outstanding performance for all types of intermolecular interactions considered in this study, although the better overall accuracy of LC-VV10 is attained at a higher computational cost associated with the inclusion of exact long-range exchange terms.

## AUTHOR INFORMATION

### Corresponding Author

*E-mail: tvan@mit.edu.

### Notes

The authors declare no competing financial interest.

## ACKNOWLEDGMENTS

This work was supported by a grant from the NSF (CHE-1058219). T.V. gratefully acknowledges a David and Lucille Packard Fellowship.

## REFERENCES

(1) Riley, K. E.; Pitoňák, M.; Jurečka, P.; Hobza, P. *Chem. Rev.* **2010**, *110*, 5023−5063.
(2) Grimme, S. *J. Comput. Chem.* **2006**, *27*, 1787−1799.
(3) Grimme, S.; Antony, J.; Ehrlich, S.; Krieg, H. *J. Chem. Phys.* **2010**, *132*, 154104.
(4) Grimme, S.; Ehrlich, S.; Goerigk, L. *J. Comput. Chem.* **2011**, *32*, 1456−1465.
(5) Eshuis, H.; Bates, J. E.; Furche, F. *Theor. Chem. Acc.* **2012**, *131*, 1084.
(6) Dion, M.; Rydberg, H.; Schröder, E.; Langreth, D. C.; Lundqvist, B. I. *Phys. Rev. Lett.* **2004**, *92*, 246401.
(7) Langreth, D. C.; Lundqvist, B. I.; Chakarova-Käck, S. D.; Cooper, V. R.; Dion, M.; Hyldgaard, P.; Kelkkanen, A.; Kleis, J.; Kong, L.; Li, S.; Moses, P. G.; Murray, E.; Puzder, A.; Rydberg, H.; Schröder, E.; Thonhauser, T. *J. Phys.: Condens. Matter* **2009**, *21*, 084203.
(8) Lee, K.; Murray, É. D.; Kong, L.; Lundqvist, B. I.; Langreth, D. C. *Phys. Rev. B* **2010**, *82*, 081101.
(9) Vydrov, O. A.; Van Voorhis, T. *Phys. Rev. Lett.* **2009**, *103*, 063004.
(10) Vydrov, O. A.; Van Voorhis, T. *J. Chem. Phys.* **2010**, *133*, 244103.
(11) Vydrov, O. A.; Van Voorhis, T. In *Fundamentals of Time-Dependent Density Functional Theory*; Marques, M. A. L., Maitra, N. T., Nogueira, F. M. S., Gross, E. K. U., Rubio, A., Eds.; Springer: Berlin, 2012; pp 443−456.
(12) Murray, E. D.; Lee, K.; Langreth, D. C. *J. Chem. Theory Comput.* **2009**, *5*, 2754−2762.
(13) Perdew, J. P.; Wang, Y. *Phys. Rev. B* **1986**, *33*, 8800−8802.
(14) Perdew, J. P.; Wang, Y. *Phys. Rev. B* **1992**, *45*, 13244−13249.
(15) Perdew, J. P.; Burke, K.; Ernzerhof, M. *Phys. Rev. Lett.* **1996**, *77*, 3865−3868.
(16) Weintraub, E.; Henderson, T. M.; Scuseria, G. E. *J. Chem. Theory Comput.* **2009**, *5*, 754−762.
(17) Vydrov, O. A.; Wu, Q.; Van Voorhis, T. *J. Chem. Phys.* **2008**, *129*, 014106.

(18) Shao, Y.; Fusti-Molnar, L.; Jung, Y.; Kussmann, J.; Ochsenfeld, C.; Brown, S. T.; Gilbert, A. T. B.; Slipchenko, L. V.; Levchenko, S. V.; O'Neill, D. P.; DiStasio, R. A., Jr.; Lochan, R. C.; Wang, T.; Beran, G. J. O.; Besley, N. A.; Herbert, J. M.; Lin, C. Y.; Van Voorhis, T.; Chien, S. H.; Sodt, A.; Steele, R. P.; Rassolov, V. A.; Maslen, P. E.; Korambath, P. P.; Adamson, R. D.; Austin, B.; Baker, J.; Byrd, E. F. C.; Dachsel, H.; Doerksen, R. J.; Dreuw, A.; Dunietz, B. D.; Dutoi, A. D.; Furlani, T. R.; Gwaltney, S. R.; Heyden, A.; Hirata, S.; Hsu, C.-P.; Kedziora, G.; Khalliulin, R. Z.; Klunzinger, P.; Lee, A. M.; Lee, M. S.; Liang, W.; Lotan, I.; Nair, N.; Peters, B.; Proynov, E. I.; Pieniazek, P. A.; Rhee, Y. M.; Ritchie, J.; Rosta, E.; Sherrill, C. D.; Simmonett, A. C.; Subotnik, J. E.; Woodcock, H. L., III; Zhang, W.; Bell, A. T.; Chakraborty, A. K.; Chipman, D. M.; Keil, F. J.; Warshel, A.; Hehre, W. J.; Schaefer, H. F., III; Kong, J.; Krylov, A. I.; Gill, P. M. W.; Head-Gordon, M. *Phys. Chem. Chem. Phys.* **2006**, *8*, 3172−3191.
(19) Zhao, Y.; Truhlar, D. G. *Theor. Chem. Acc.* **2008**, *120*, 215−241.
(20) Chai, J.-D.; Head-Gordon, M. *Phys. Chem. Chem. Phys.* **2008**, *10*, 6615−6620.
(21) Řezáč, J.; Riley, K. E.; Hobza, P. *J. Chem. Theory Comput.* **2011**, *7*, 2427−2438.
(22) Řezáč, J.; Riley, K. E.; Hobza, P. *J. Chem. Theory Comput.* **2011**, *7*, 3466−3470.
(23) Marshall, M. S.; Burns, L. A.; Sherrill, C. D. *J. Chem. Phys.* **2011**, *135*, 194102.
(24) de Lange, K. M.; Lane, J. R. *J. Chem. Phys.* **2011**, *134*, 034301.
(25) McMahon, J. D.; Lane, J. R. *J. Chem. Phys.* **2011**, *135*, 154309.
(26) Hujo, W.; Grimme, S. *J. Chem. Theory Comput.* **2011**, *7*, 3866−3871.
(27) Goerigk, L.; Kruse, H.; Grimme, S. *ChemPhysChem* **2011**, *12*, 3421−3433.
(28) Sherrill, C. D.; Takatani, T.; Hohenstein, E. G. *J. Phys. Chem. A* **2009**, *113*, 10146−10159.